View metadata, citation and similar papers at core.ac.uk

brought to you by CORE

東北大学機関リポジトリ
TOUR
Tohoku University Repository

Resonator combined with a piezoelectric actuator for chemical analysis by force microscopy

著者	小野　崇人
journal or publication title	Review of scientific instruments
volume	78
number	6
page range	063709-1-063709-4
year	2007
URL	http://hdl.handle.net/10097/35801

doi: 10.1063/1.2748394

Resonator combined with a piezoelectric actuator for chemical analysis by force microscopy

Yusuke Kawai,[a] Takahito Ono, and Masayoshi Esashi
Graduate School of Engineering, Tohoku University, Sendai 980-8579 Japan

Ernst Meyer
Department of Physics, University of Basel, Switzerland

Christoph Gerber
NCCR National Center of Competence for Nanoscience, University of Basel, Switzerland

(Received 6 February 2007; accepted 21 May 2007; published online 27 June 2007)

A high frequency silicon resonator for dynamic scanning force microscopy is combined with an integrated piezoelectric actuation element for large displacements. A high resonance frequency is required for imaging on the nanometer scale, and a large displacement is needed for the chemical analysis of the material at the end of the probe. The small piezoelectric resonator is formed at the end of a long piezoelectric actuator using a silicon micromachining technology. The resonator can be oscillated at 96.4 kHz, and the actuator generates a maximum displacement of 15 μm at the end of the probe. The dynamic-mode scanning force microscopy capability, using the integrated piezoelectric resonator, is demonstrated on a 2 μm pitch Au grating. © *2007 American Institute of Physics.* [DOI: 10.1063/1.2748394]

I. INTRODUCTION

Scanning force microscopy (SFM) is a well-established technique to obtain topography and various physical and chemical properties of surfaces on the nanometer scale.[1] In particular, the observation of atomic resolution and manipulation of atoms or molecules are essential methods.[2,3] An important challenge in this field is the chemical identification of individual molecules or atoms. To achieve this goal, imaging of a given surface with atomic resolution and subsequent chemical analysis of the selected single molecule or atom is needed. This technique gives the opportunity to map atom distributions and to determine the composition of molecules on the surface. Up to now, scanning atom probe with an aperture has been employed to analyze atoms on a tapered sample.[4] Recently, the analysis of surfaces has been demonstrated by a combination of a time-of-flight mass analyzer (TOF-MA) and scanning tunneling microscopy (STM).[5,6] STM techniques are limited to conductive materials, where SFM has no such boundary conditions, e.g., in its versatile application from insulators to biomolecules. The combination of TOF-MA and SFM (Refs. 7 and 8) is advantageous for imaging and chemical analysis of surfaces with the potential of atomic resolution. In this TOF-SFM, the cantilever probe ionizes particles picked up from the surface. In order to emit the atoms for mass analysis, an extraction electrode is placed close to the tip of the probe. The cantilever is bent by thermal actuation for directing its tip position to the front of the extraction electrode.[8] This integration in the probe provides low voltage operation of the field-assisted ion emission. The probe can precisely return to its original position for further imaging of the surface. This switching operation requires a large actuation of the probe. The stiffness of the actuator must be reduced to satisfy this requirement because the generated power of the miniaturized actuator has to be limited. On the other hand, for the nondestructive observation of surfaces, dynamic modes of SFM including tapping mode, noncontact (NC) mode, and alternating current (ac) mode have been employed. In general, several hundred kilohertz of a resonance frequency is required for achieving a high resolution and stability in imaging with conventional dynamic SFM.

Regarding the actuator for TOF-SFM, a nonthermal type actuator has the benefit that a smaller amount of heat is generated. Since the thermal migration of the manipulated molecules or atoms on the tip is reduced, the probability of emission of atoms during the positioning of the tip in front of the extraction electrode is increased. In comparison with the thermal actuation method, piezoelectric actuation has the additional benefit that the probe can be driven faster. The integration of piezoelectric transducer (PZT) thin film microactuators with unimorph configuration into a SFM probe has been reported.[9,10] The unimorph actuator, consisting of a thin Si cantilever and a PZT thin film, offers a large displacement because PZT has a large piezoelectric constant and high electromechanical coupling coefficient. In addition, the unimorph configuration can act as a force sensor for detecting the vibration of the probe based on the piezoelectric effect. Piezoelectric actuators as well as piezoelectric sensors can be integrated by conventional microfabrication technology. Therefore, an optical sensing system is not needed, which makes the measurement system simple and provides the capability of operating in various environments.

In this study, we have developed a SFM probe, where a

[a]Electronic mail: kawai@mems.mech.tohoku.ac.jp

 © 2007 American Institute of Physics

Downloaded 02 Dec 2008 to 130.34.135.83. Redistribution subject to AIP license or copyright; see http://rsi.aip.org/rsi/copyright.jsp

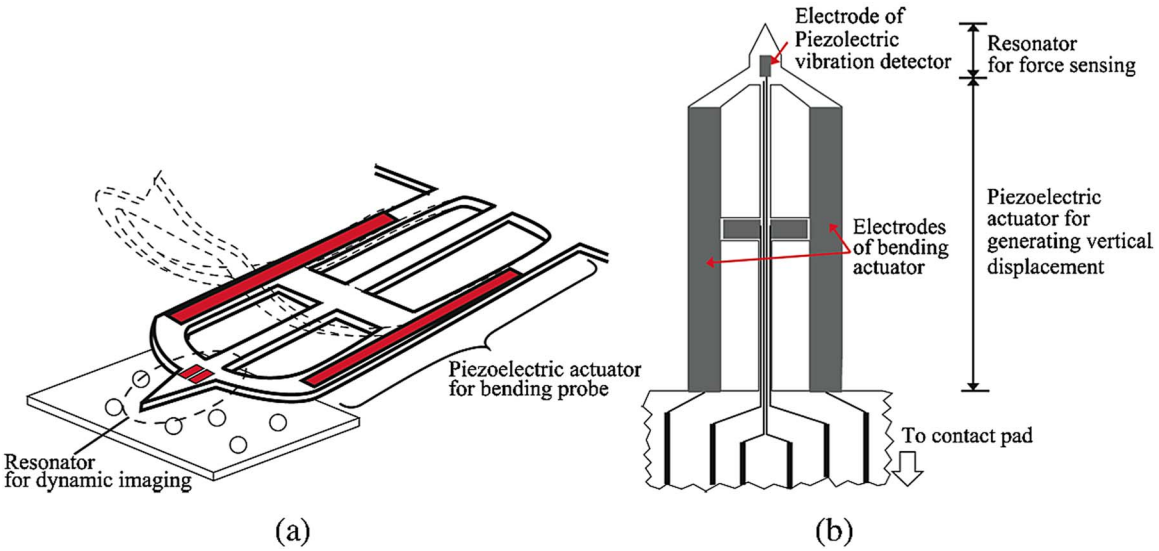

FIG. 1. (Color online) (a) Schematic figure of the resonator integrated with a piezoelectric actuator picking up material to be analyzed by TOF-MA. (b) Top view of the probe design.

piezoelectric resonator for surface imaging is combined with a piezoelectric unimorph actuator for bending the probe. This probe consists of a short piezoelectric resonator at the end of the actuator for topographic imaging by dynamic SFM and a long piezoelectric actuator to position the probe for a time-of-flight mass analysis. The resonance frequency of the short resonator is well separated from the resonance frequency of the long actuator. Here, the design, fabrication, and characterization of the probe with the integrated piezoelectric unimorph actuator are presented. Furthermore, imaging of surface topography based on dynamic SFM is demonstrated.

II. DESIGN AND FABRICATION OF ACTUATOR-INTEGRATED PROBE

As shown in Figs. 1(a) and 1(b), the probe consists of a short resonator for imaging and a long actuator for generating large, vertical displacements at the end of the probe. A piezoelectric vibration sensor is attached to the support of the resonator for dynamic SFM. Two piezoelectric unimorph beams, which support the resonator, can serve as actuators. A PZT thin film of unimorph structure is grown across the whole area of the metallized probe. The integrated sensor and piezoelectric actuator have a common lower electrode and individual upper electrodes. In scanning mode, the resonator, which has a higher resonance frequency than that of the actuator, is vibrated by the external piezoactuator.

Figure 2 shows the fabrication process of the probe. The starting material is a silicon-on-insulator (SOI) wafer with a 1.5-μm-thick (100)-oriented Si top layer and a 1.0-μm-thick buried oxide layer (a). A silicon dioxide layer with a thickness of 160 nm was formed by thermal oxidation to avoid diffusion of Ti into the Si device layer. A 50-nm-thick Ti film, a 100-nm-thick Pt film, and, subsequently, a 250-nm-thick PZT film were deposited on the oxide layer using magnetron multitarget sputtering at 315 °C. Next, the deposited PZT film was crystallized by rapid thermal annealing (RTA) at 600 °C for 10 min with a temperature rising rate of 100 °C/s (b). The x-ray diffraction measurement of the polycrystalline PZT thin film exhibits both peaks of (100) and (111). After photolithography, Cr and Au films with thicknesses of 30 and 100 nm, respectively, were deposited by sputtering and patterned by lift-off processes to form the top electrodes for the piezoelectric sensor and actuator (c). The PZT film was patterned by wet etching in a mixture solution of HF, HCl, and H_2O (0.2:30:70 by volume[11]) at 56 °C in order to make electrical contacts with the lower electrode (d).[12] The PZT layer, lower electrode layer, and top Si layer of SOI were etched for making the probe pattern using a fast atom beam (FAB) of SF_6 gas with a 4-μm-thick photoresist mask. The FAB, which was provided by neutralized accelerating ions, can etch an insulating material with less influence of build-in charges. The etching rate of the PZT film was 30 nm/min using the SF_6 FAB with 3 kV of acceleration voltage at room temperature (e). Finally, the backside of the wafer and buried oxide layer were etched by deep reactive ion etching (DRIE), and the probe structures were released (f). Figure 3 shows the scanning electron microscope (SEM) image of the fabricated probe with a total

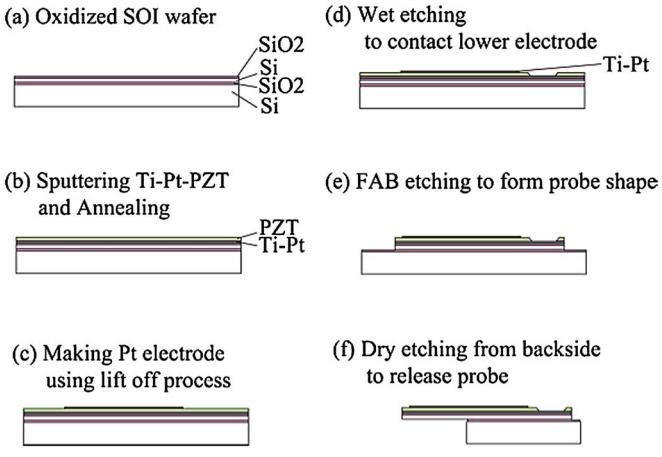

FIG. 2. (Color online) Schematic fabrication process of the probe by silicon micromachining technology.

Downloaded 02 Dec 2008 to 130.34.135.83. Redistribution subject to AIP license or copyright; see http://rsi.aip.org/rsi/copyright.jsp

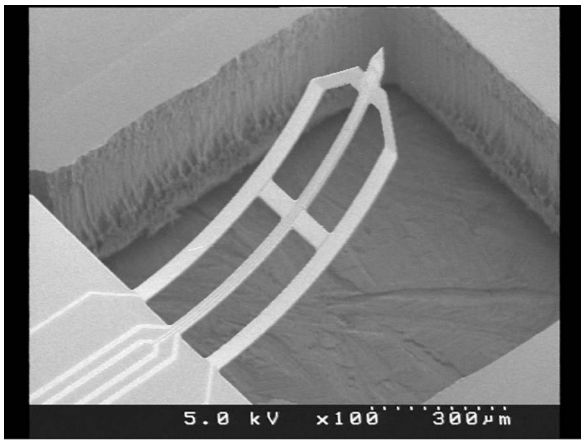

FIG. 3. SEM image of the fabricated probe with a length of 750 μm.

length of 750 μm, where the length of the resonator is 100 μm. The probe bends with an angle of 45° at the probe end due to thermal and internal stresses after the deposition and crystallization processes of the PZT thin film at a high temperature. The processed PZT thin film exhibits a tensile stress of approximately 160 GPa.

III. CHARACTERIZATION OF INTEGRATED PIEZOELECTRIC ACTUATOR

The performance of the PZT actuator regarding the displacement of the fabricated probe was characterized. In order to make electrical contact, metal wires were connected to the metal pads of upper and lower electrodes using a conductive glue. In this experiment, only one actuator of the two beams could be driven because of electrical shortage between the upper and lower electrodes. The piezoelectric actuator generates a static displacement of approximately 15 μm in vertical direction with respect to the substrate at an applied voltage of 5 V (an electric field of 200 kV/cm) to a 250-nm-thick PZT film. At an application voltage higher than 5.5 V, electrical breakdown in the PZT film has been observed.

Figure 4 shows the measured displacement at the probe end as a function of the applied dc voltage. The measurement was performed using a laser displacement sensor equipped with an optical microscope. Figure 4 shows the measured

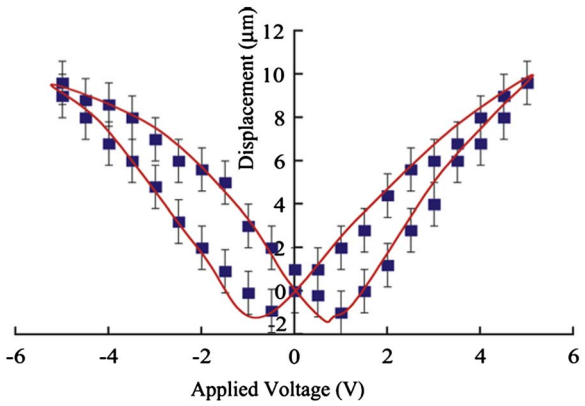

FIG. 4. (Color online) Measured displacement of the piezoelectric actuator as a function of the applied voltage.

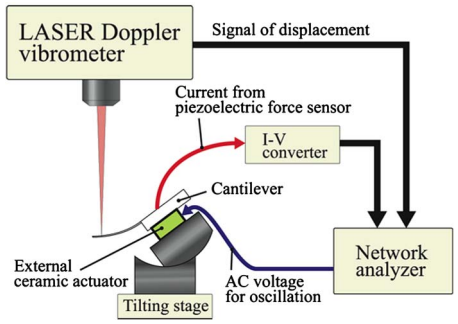

FIG. 5. (Color online) Schematic figure of the experimental setup, where frequency characteristics of the probe are determined.

displacement plotted against the applied voltage, which exhibits the typical ferroelectric hysteresis behavior. At voltages of 0.8 and −0.8 V, the repoling of polarization in the PZT film is observed. This switching electric field, the coercive field strength, is approximately 40 kV/cm. From the characteristics of the probe actuation, the calculated piezoelectric constant d_{31} of this PZT thin film is found to be approximately −150 pm/V. The known bulk value of the piezoelectric constant of PZT is −360 pm/V. If the two piezoelectric actuators are driven, larger displacements will be obtained.

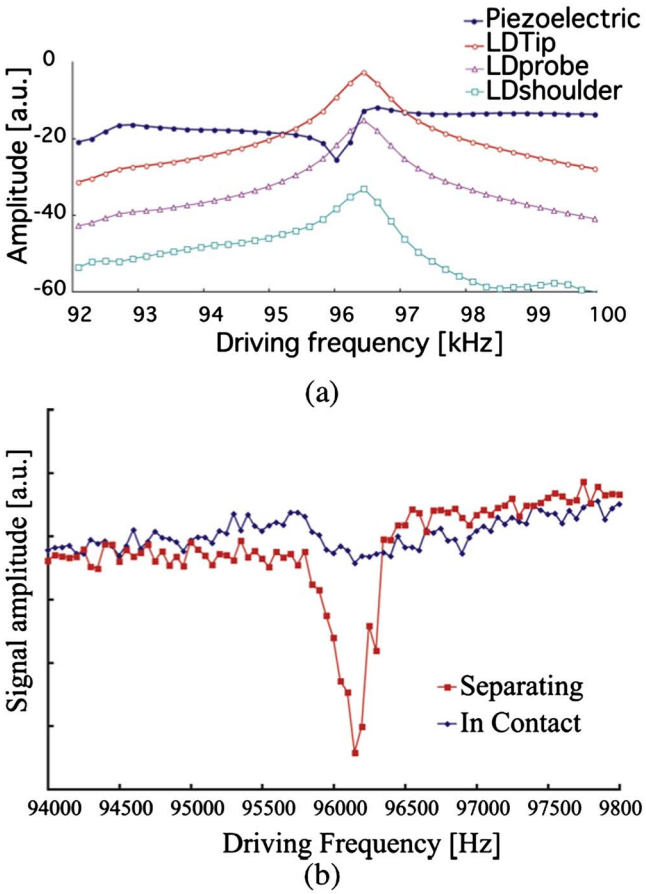

FIG. 6. (Color online) (a) Excitation spectrum of the resonator. Open circles are measured by the laser Doppler displacement sensor. Filled circles are measured by the integrated piezoelectric detector. (b) Amplitude comparison of the piezoelectric force sensor in contact to the surface and out of contact.

Downloaded 02 Dec 2008 to 130.34.135.83. Redistribution subject to AIP license or copyright; see http://rsi.aip.org/rsi/copyright.jsp

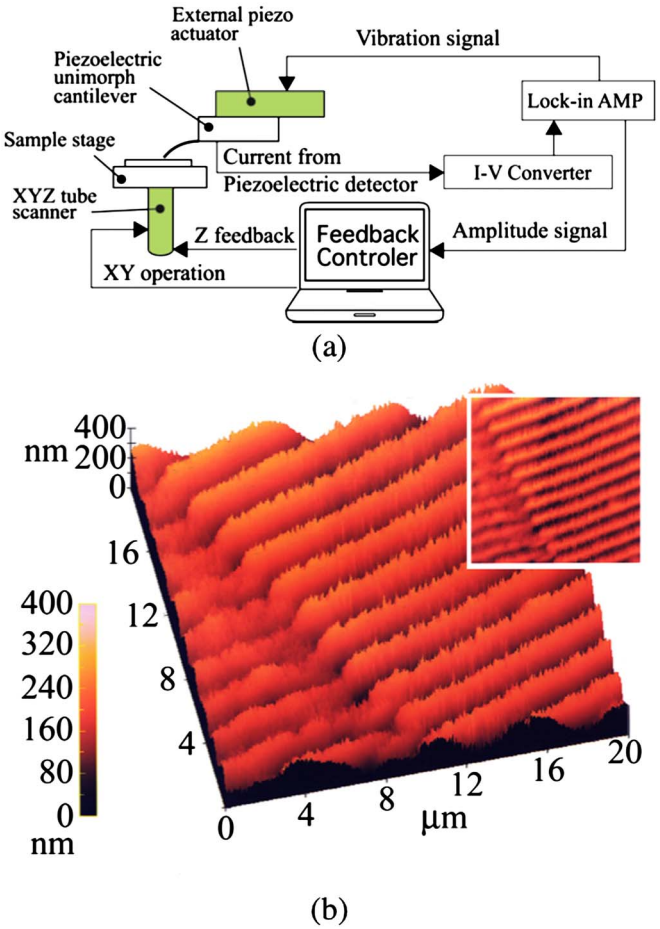

FIG. 7. (Color online) (a) Block diagram of the experimental setup of the dynamic force microscope in the intermittent mode. (b) SFM image of the 2 μm pitch Au grid using the piezoelectric resonator.

IV. IMAGING EXPERIMENT WITH PIEZOELECTRIC DETECTION

Dynamic SFM using the integrated piezoelectric resonator at the end of the actuator is demonstrated. The vibration is measured to identify modes of the resonator with an integrated piezoelectric detector and a laser Doppler vibrometer. The schematic figure of the experimental setup for measuring the resonance frequency is shown in Fig. 5. Excited by an external piezoactuator, the vibration amplitude, measured by the integrated piezoelectric detector, is compared with the actual vibration amplitude, measured by the laser Doppler vibrometer. Amplified by a current-voltage converter, the vibration signals were processed with a network analyzer. Figure 6(a) shows the fundamental flexural mode of the resonance peak at 96.4 kHz. The signal spectrum of the piezoelectric detection shows an antiresonance peak and a resonance peak at 96.1 and 96.4 kHz, respectively. As shown in Fig. 6(b), the vibrating amplitude at the antiresonance frequency disappears when the probe is in contact with the surface. This vibration mode is employed for SFM using a slope detection method. The block diagram of the setup for dynamic SFM imaging is shown in Fig. 7(a). The resonator is oscillated by an external piezoactuator at 96.2 kHz. An *XYZ* three-axis piezotube scanner is employed as a sample stage. The signal from the integrated piezoelectric resonator is detected using a lock-in amplifier, where the amplitude signal is used as a feedback to the piezotube scanner.

Figure 7(b) shows the tapping mode SFM image of a Au grid with a scanning area of 20×20 μm^2. The height, width, and pitch of the grid are 250 nm, 1 μm, and 2 μm, respectively.

In summary, a novel device is fabricated using silicon micromachining technology. The combination of a high frequency resonator with a piezoelectric actuator allows fast and reliable switching from an imaging to an analysis mode by TOF-MA, paving the way to chemical SFM.

ACKNOWLEDGMENTS

This work is supported in part by Future Medical Engineering based on Bionanotechnology 21st century COE Program, Tohoku University and also supported in part by a Grant-in Aid for Scientific Research from the Japanese Ministry of Education, Culture, Sports, Science and Technology of Japan. A part of this work was performed at the Micro/nanomachining Research Education Center, Tohoku University. Further funding was provided by the National Center of Competence in Research on Nanoscale Science and the Swiss National Science Foundation.

[1] G. Binnig, H. Rohrer, Ch. Gerber, and E. Weibel, Phys. Rev. Lett. **56**, 930 (1986).
[2] F. J. Giessibl, Science **267**, 68 (1995).
[3] N. Oyabu, O. Custance, I. Yi, Y. Sugawara, and S. Morita, Phys. Rev. Lett. **90**, 176102 (2003); Y. Sugimoto, P. Pou, M. Abe, P. Jelinek, R. Perez, S. Morita, and O. Custance, Nature (London) **446**, 64 (2007).
[4] O. Nisikawa *et al.*, Appl. Surf. Sci. **146**, 398 (1999).
[5] Y. Ding, R. Micheletto, H. Hanada, T. Nagamura, and S. Okazaki, Rev. Sci. Instrum. **73**, 3227 (2002).
[6] J. C. H. Spence, U. Weierstall, and W. Lo, J. Vac. Sci. Technol. B **14**, 1587 (1996).
[7] A. Wetzel, A. Socoliuc, E. Meyer, R. Bennewitz, E. Gnecco, and C. Gerber, Rev. Sci. Instrum. **76**, 103701 (2005).
[8] D. Lee, A. Wetzel, R. Bennewitz, E. Meyer, M. Despont, P. Vettiger, and C. Gerber, Microelectron. Eng. **67–68**, 635 (2003).
[9] S. Watanabe and T. Fujii, Rev. Sci. Instrum. **67**, 3898 (1996).
[10] C. Lee, T. Itoh, and T. Suga, Sens. Actuators, A **72**, 179 (1999).
[11] J. Baborowski, J. Electroceram. **12**, 33 2004.
[12] J. G. Smit, K. Fujimoto, and V. F. Kleptsyn, J. Micromech. Microeng. **15**, 1285 (2005).

Downloaded 02 Dec 2008 to 130.34.135.83. Redistribution subject to AIP license or copyright; see http://rsi.aip.org/rsi/copyright.jsp